

Phonon softening: “keyhole” into dynamic stripe-phase

Sergei I. Mukhin

Theoretical Physics Department, Moscow Institute for Steel and Alloys, Leninskii pr. 4,
119991 Moscow, Russia

Running title: soft phonons and dynamic stripes

Keywords: high- T_c cuprates, in-plane optical phonon modes, phonon self-energy, meandering stripes, on-stripe spinless fermionic holes

The highly distinctive phonon self-energy dependences on the wave vector, calculated respectively for the static and dynamic stripe phase models of the underdoped cuprates are presented. The negative values of the real part of the on-stripe holes polarization loop lead to appearance of localized vibration states in the presence of well-separated stripes, relevant for underdoped cuprates. The localized modes split below the bare optical phonon frequencies exhibiting strong “softening effect”. The calculated gap between localized and propagating phonon frequencies is practically doping independent in accord with the recent neutron measurements. The derived wave vector dependence of the phonon softening nicely coincides with anomalously shallow experimental curve in high- T_c cuprates when stripe meandering is taken into account. Co-centering of the theoretical and experimental curves implicates on-stripe holes statistics.

PACS numbers: 64.60.-i, 71.27.+a, 74.72.-h, 75.10.-b

I. INTRODUCTION AND MAIN RESULTS

The independence on doping of the amount of softening of the optical phonon modes measured by neutrons in high- T_c cuprates^{1,2}, concomitant with the linear doping-dependence of the modes intensity, points to a local on-stripe character of the softening effect³. The latter effect may arise due to coupling of the in-plane optical Cu-O stretching modes (LO) to the holes populating stripes. In this paper, in order to explore the effect theoretically, the stripes are considered as one-dimensional (1D) “metallic rivers of doped holes”⁴. Spatially localized vibrations are found, that split below the bare phonon band in the stripe-phase, as was proposed earlier⁵. The source of localization of the lattice vibrations is the phonon self-energy, significantly space-modulated in the presence of the on-stripe holes. It is shown that this self-energy plays a role of attractive localizing potential for the phonon quasi-particles, provided that its real part is negative and has sufficiently high absolute value. The latter depends on the wave-vector in the direction along the stripes. In this direction the translational symmetry of the crystal lattice is preserved. It is demonstrated here that phonon self-energy, calculated from the standard Feynman diagram Fig.B, cannot lead to the peculiar flat momentum dependence of the optical mode softening measured by neutron scattering in La-based high- T_c cuprates, see filled circles in Fig.B. As it is apparent from Fig.B, a rather poor agreement with experimental data is obtained for the case of the holes moving along 1D static stripes (dash-dotted line), as well as for the case of the holes moving three(two)-dimensionally (dotted line). Miraculously, inclusion into phonon self-energy of the overdamped long wavelength stripe-meandering propagator, see Fig. B, leads to impressive coincidence of the theoretical phonon softening curve (solid line) in Fig. B, with the experimental data (filled circles). Besides the flat momentum dependence of the modes softening, the co-centering of the experimental and theoretical curves is also important. Position of zero along the Q -axis of the theoretical curve depends on the Fermi momentum of the on-stripe holes. This leads to important observation that the theoretical phonon dispersion curve coincides with the experimental one, provided that the underlying 1D “Fermi momentum” along stripes is twice the value predicted in the weak-coupling scheme. This discrepancy may be tolerated if one assumes the holes inside stripes to be spinless. Incidentally, the energy-integrated ARPES data⁶ exhibit flat parallel pieces enclosing high spectral weight region in the Brillouin zone (the “holy cross” picture), that resemble 1D “Fermi surface” of the

on-stripe holes, but with Fermi momentum value corresponding to the weak-coupling scheme. This may indicate that “spin-dressed” holes rather than spinless are involved in the ARPES measurements.

Section II contains derivation of the dynamic elasticity equations for the 2D plane with periodic stripes. Section III uses straightforward mapping of the elasticity equations onto Schrödinger equations for a quantum particle in the periodic Dirac’s haircomb potential. Localized solutions describe “softened phonon” modes. In Sections IV and V different dependences of the phonon self-energy on the wave vector along the stripes are calculated for static and meandering 1D stripes respectively. Section VI contains description of the model parameters found by fitting the theoretical curves to experimental data, and concludes with discussion of the main results briefly reviewed above. Some lengthy analytical expressions are located in the Appendices A and B.

II. 2D LATTICE DYNAMICS IN THE STRIPE-PHASE

Elastic behavior of 2D quadratic lattice (modeling CuO planes in cuprates) is considered in the continuum media approximation. Corresponding expression for the elastic energy density reads (see e.g.⁷):

$$\varepsilon(\vec{r}) = \frac{1}{2}(2\mu + \lambda)(u_{11}^2 + u_{22}^2) + \lambda u_{11}u_{22} + 2\mu u_{12}^2. \quad (1)$$

here λ is Lamé constant; μ is shear modulus. The strain tensor components $u_{ij} =$, $i, j = 1, 2$ are :

$$u_{ij} = \frac{1}{2}(\partial_i u_j + \partial_j u_i + \partial_i u_l \partial_j u_l) \quad (2)$$

where u_x , u_y are the in-plane local displacements of the lattice; $\partial_i \equiv \partial/\partial x_i$ and coordinates x_i belong to the plane $\{x, y\}$.

Assume that stripes are oriented along y -axis in the $\{x, y\}$ plane. Hence, in the static picture they form a periodic array with a period $b \sim 1/x_h$ along the x -axis, where x_h is the concentration of doped holes in the Cu-O plane counted from the insulating state $x_h = 0$. Then, translation invariance along y -axis is preserved and therefore vibrations keep y -component of quasi momentum Q . Corresponding dynamic elasticity equations in the mixed momentum-coordinate representation take the form:

$$\begin{aligned} [\rho\omega^2 - \mu Q^2 + (\mu + K)\partial_{xx}^2 - \pi_1(Q, \omega)p(x)] u_x + iKq\partial_x u_y &= 0 \\ [\rho\omega^2 - (\mu + K)Q^2 + \mu\partial_{xx}^2 - \pi_2(Q, \omega)p(x)] u_y + iKq\partial_x u_x &= 0 \end{aligned} \quad (3)$$

where ρ is the lattice density of mass and $K = \lambda + \mu$ is the lattice compression modulus in the absence of doped holes. Here ω is brought by the Fourier transformation along the time axis t :

$$u_x = u_x(x) \exp\{iQy - i\omega t\}; u_y = u_y(x) \exp\{iQy - i\omega t\}, \quad (4)$$

The Q, ω, x -dependent phonon self-energy is included in the dynamics equations (3) in the simplest possible way via the terms $\pi_i(Q, \omega)p(x)$. Here Q, ω -dependence is due to hole motion along stripes inside the “metallic rivers of charge” separating antiphased antiferromagnetic domains in the “canonical” stripe phase pattern^{9,4}. A model simplifies the general tensorial self-energy $\pi_{ij}(Q, \omega, x)$ with a diagonal matrix, maintaining essential physics of phonon localization, but avoiding intractable algebra:

$$\pi_{xy} = 0; \pi_{xx} = \pi_1(Q, \omega)p(x), \pi_{yy} = \pi_2(Q, \omega)p(x); \quad (5)$$

where a “tight binding” approximation is used to mimic periodic x -dependence in the direction perpendicular to the stripes:

$$p(x) = \sum_n \delta(x + bn) \quad (6)$$

Here n enumerates the stripes and b is the interstripe period. This approximation looks reasonable for underdoped cuprates, since according to e.g.⁸ the number of doped holes/per double-period $2a$ along a stripe is fixed to one, and therefore the interstripe period $b = a/2x_h \gg a$ in the low hole-doping limit $x_h \ll 1$ for a square lattice. In the limit of vanishing electron-phonon coupling $\pi_i(Q, \omega) \rightarrow 0$, the system (3) smoothly transforms into a standard system of dynamic equations for 2D isotropic elastic media that possesses two phonon branches: longitudinal and transverse⁷, provided that the following condition is fulfilled:

$$\pi_1(Q, \omega) = \pi_2(Q, \omega)(\mu + K)/\mu \equiv \pi(Q, \omega). \quad (7)$$

Straightforward calculations show that imaginary parts of $\pi_{1,2}$ merely result in a weak damping of the vibration modes. This effect will be neglected here, and only real part $Re\pi(Q, \omega)$ that results in softening of the vibration modes will be retained.

Diagrammatic form of the electronic (hole) polarization loop $\pi(Q, \omega)$ contributing to the phonon self-energy is exhibited in Fig.B. Here the dot is electron(hole)-lattice coupling vertex, the thin lines are Green's functions $G(p, \epsilon)$ of the 1D hole possesing momentum p along the stripe:

$$G^R(p, \epsilon) = \frac{1}{\epsilon - \tilde{\epsilon}(p) + i\tau_p^{-1}}; \quad \tilde{\epsilon}(p) \equiv \epsilon(p) - \epsilon_F = \epsilon_F(p^2 - 1) \quad (8)$$

In Fig. B the wavy line is added. It represents concomitant inelastic forward scattering event with small momentum transfer ($q \ll Q \sim 2p_F$) due to stripe vibrations described by a propagator $g(q, \omega)$. A weak-coupling quasi classical description of the effect of meandering on a hole motion along the stripe is sketched in Appendix B. The superscript R signifies retarded Green's function, ϵ_F is 1D “Fermi energy” (chemical potential) of the on-stripe mobile holes, and momentum p is normalized by 1D Fermi-momentum p_F ; τ_p is particle life-time. A parabolic dispersion $\epsilon(p)$ is chosen for the mobile on-stripe holes for simplicity. A particular expression for the stripe vibration propagator $g(q, \omega)$ will be elucidated below using best fit to the experimental data of Pintschovius et.al.².

III. LOCALIZED VIBRATIONS IN A “HAIRCOMB” POTENTIAL

By their mathematical structure equations (3) map onto a set of the two coupled Schrödinger equations for a quantum particles of “masses” $(\mu + K)^{-1}/2$ and $\mu^{-1}/2$ in the periodic Dirac's haircomb potentials $\propto \pi_i p(x)$. It is important to mention that this “potentials” are attractive when $Re\pi_i p(x) < 0$. Hence, the real parts of the polarization loops in Figs.B,B have to be negative in order to cause splitting off a narrow band of the localized vibrations below the bottom of the bare propagating phonons band (the “softening effect”). Corresponding Bloch solutions in the periodic potential obey the following quasi periodicity conditions at the adjacent intervals along the x - axis:

$$\begin{aligned} \vec{u}(x) &\equiv \{u_x(x), u_y(x)\} = \vec{A} \exp\{\nu x\} + \vec{B} \exp\{-\nu x\}; \quad 0 \leq x \leq b; \\ \vec{u}(x) &= \exp\{ikb\} [\vec{A} \exp\{\nu x\} + \vec{B} \exp\{-\nu x\}]; \quad b \leq x \leq 2b. \end{aligned} \quad (9)$$

Here quasi-momentum k is parallel to the x -axis (i.e. perpendicular to the stripes direction) and spans the interval $[-\pi/b, \pi/b]$. The case of real ν corresponds to vibrations localized in the vicinity of the stripes. The two-component vectors \vec{A}, \vec{B} are defined as:

$$\vec{A} \equiv \{A_x, A_y\}; \quad \vec{B} \equiv \{B_x, B_y\} \quad (10)$$

Continuity of the solution $\vec{u}(x)$ at the point $x = b$ together with conditions for the first derivatives following from Eqs. (3):

$$\begin{aligned} (\mu + K) [\partial_x u_x(b + 0) - \partial_x u_x(b - 0)] - \pi_1 u_x(b) &= 0; \\ \mu [\partial_x u_y(b + 0) - \partial_x u_y(b - 0)] - \pi_2 u_y(b) &= 0, \end{aligned} \quad (11)$$

lead to a single eigenvalue equation (due to a simplifying relation (7)):

$$\cos(kb) = \cosh(\nu b) + \frac{\pi(Q, \omega)}{2\nu(\mu + K)} \sinh(\nu b); \quad (12)$$

This equation determines spectrum of the wave vector $\nu(k)$.

Substitution of the Bloch-wave (9), taken in the interval $0 < x < b$, into Eqs. (3) leads to the following system of algebraic homogeneous equations:

$$\begin{cases} [\rho\omega^2 - \mu Q^2 + (\mu + K)\nu^2] A_x + iK\nu Q A_y = 0; \\ iK\nu Q A_x + [\rho\omega^2 - (\mu + K)Q^2 + \mu\nu^2] A_y = 0. \end{cases} \quad (13)$$

A dispersion $\omega(Q, k)$ is found by solving determinant equation of the system (13):

$$(\rho\omega^2 - \mu(Q^2 - \nu^2))(\rho\omega^2 - (\mu + K)(Q^2 - \nu^2)) = 0 \quad (14)$$

Solutions of (14) with $\nu = \nu(k)$ result in two branches of dispersion $\omega_{t,L}(Q, k)$:

$$\omega_{t,L}^2(Q, k) = c_{t,L}^2(Q^2 - \nu^2(k)); \quad (15)$$

Here $c_{t,L}$ are sound velocities of 2D elastic media⁷:

$$c_t^2 = \mu/\rho; \quad c_L^2 = (\mu + K)/\rho. \quad (16)$$

Without electron-phonon coupling the corresponding unperturbed branches are:

$$\omega_{t,L}^{02}(Q, k) = c_{t,L}^2(Q^2 + k^2); \quad (17)$$

since at $\pi(Q, \omega) \rightarrow 0$ the eigen values of momentum ν , that are solutions of Eq. (12), are purely imaginary: $\nu = ik$, and correspond to the propagating vibrations. It is known from the ordinary quantum mechanics that localized states, i.e. in the present case vibrations $u_{x,y}(x)$ with real wave-vector ν , have “energies” below the bottom of the propagating band. Indeed, it is apparent from a direct comparison of Eqs. (15) and (17), that for real $\nu(k)$: $\omega_{t,L}(Q, k) < \omega_{t,L}^{02}(Q, k)$. This, in turn, signifies a phonon softening effect due to on-stripe electron-phonon coupling. Equation (12) possesses real solutions $\nu(k)$ in the whole interval $-\pi \leq kb \leq \pi$ when $Re\pi(Q, \omega) < 0$ and $|Re\pi(Q, \omega)|b/(\mu + K) > 4$. An imaginary solution $i\nu$ appears first time when $\nu(k)$ reaches zero. In this case equation (12) reads:

$$\cos(kb) = 1 - \frac{|\pi(Q, \omega)|b}{2(\mu + K)}. \quad (18)$$

This equality can be satisfied when $0 \leq |\pi(Q, \omega)|b/(\mu + K) \leq 4$. (Here and below the imaginary part $Im\pi(Q, \omega)$, leading to weak damping of the modes, is neglected.) Then, the lowest-value imaginary solutions $i\nu$ appear in the subinterval of k 's: $\arccos\{1 - |Re\pi(Q, \omega)|b/(2(\mu + K))\} \leq kb \leq \pi$. They correspond to dispersion $\omega(Q, k)$ merging with propagating phonon band $\omega^0(Q, k)$. Finally, when $Re\pi(Q, \omega) > 0$ all solutions $\nu(k)$ are imaginary.

In the low doping limit, assuming $|Re\pi|b/(\mu + K) \propto x_h^{-1} \gg 1$, the decay wave vector $\nu = \nu(k)$ spans a narrow band between the bounds ν_{\pm} when k spans the interval $(-\pi/b, \pi/b)$:

$$\nu_{\pm} = -\frac{Re\pi(Q, \omega)}{2(\mu + K)} \left(1 \mp 2 \exp \left\{ \frac{Re\pi(Q, \omega)b}{2(\mu + K)} \right\} \right) \quad (19)$$

Importantly, it follows from Eq. (19) that in the strong coupling limit $|Re\pi|b/(\mu + K) \gg 1$ the wave-vector $\nu(k) \approx \text{const}$, since in this limit the exponentially small second term in the right hand side of Eq. (19) can be neglected. This makes softening independent of the hole doping concentration x_h (involved in (19) only via interstripe period b), in accord with the experiments in high- T_c cuprates^{1,2}. Substituting (19) into Eq. (15) one finds the following generalized relations:

$$\Delta\omega_{t,L}(Q, k) \approx -\frac{c_{t,L}^2}{2\omega_{t,L}^{02}(Q, k)} \left(\frac{Re\pi(Q, \omega_L)}{2(\mu + K)} \right)^2. \quad (20)$$

where $\Delta\omega_{t,L}(Q, k) \equiv \omega_{t,L}(Q, k) - \omega_{t,L}^0(Q, k)$. Relations (20) are remarkable, the softening amount $\Delta\omega_{t,L}(Q, k)$ of the in-plane phonon modes is expressed via the self-energy correction to the phonon Green's function arising from the on-stripe hole-phonon coupling. The self-energy is given by the polarization loop $\pi(Q, \omega)$, that characterizes properties of the holes moving along the valley of a single stripe. As will be demonstrated below, the flat Q -dependence of the modes softening measured experimentally^{1,2} leaves narrow room for the different choices of statistics and dynamical characteristics of the mobile on-stripe holes. Thus, relations (20) open an exclusive “keyhole” into the nature of stripes in strongly correlated electron systems, and in particular, in the underdoped high- T_c cuprates.

IV. PHONON SELF-ENERGY: 1D HOLES INSIDE STATIC STRIPES

First, consider static stripes and use the standard methods¹⁰ to find expression for polarization loop of the 1D on-stripe holes (see Fig. B):

$$\begin{aligned} \pi(Q, i\omega) = & \frac{g^2}{2\pi^2} \int_{-\infty}^{\infty} d\epsilon \int dp \{ ImG^R(p, \epsilon)G^A(p + Q, \epsilon - i\omega) + \\ & ImG^R(p + Q, \epsilon)G^R(p, \epsilon + i\omega) \} \tanh\left(\frac{\epsilon}{2T}\right); \omega = 2\pi nT, n = 0, \pm 1, \dots \end{aligned} \quad (21)$$

Here g is electron-phonon coupling constant and $G^{R,A}$ are retarded and advanced versions of the Green's function (8), ω is the Matsubara frequency. After an analytic continuation into real axis of ω of the expression (21) and separation of the real part, one finds the inverse localization length $\nu(k) \approx \nu(Q, \omega)$ using eqs. (19) and (21):

$$\begin{aligned} \nu(Q, \omega) = & -\gamma \frac{1}{2\pi} \int_{-\infty}^{\infty} d\epsilon \int dp \{ ImG^R(p, \epsilon)ReG^R(p + Q, \epsilon - \omega) + \\ & ImG^R(p + Q, \epsilon)ReG^R(p, \epsilon + \omega) \} \tanh\left(\frac{\epsilon}{2T}\right); \end{aligned} \quad (22)$$

$$\gamma = \frac{g^2\hbar}{4\epsilon_F(\mu + K)p_FV_0} \sim 1. \quad (23)$$

Here T is the temperature and V_0 is the volume of the unit cell. All energies are expressed in units of ϵ_F . As will become apparent below, a reasonable fit to experimental data can be obtained neglecting T as compared with τ_p^{-1} . The analytic expression for $\nu(Q, \omega)$ derived in this limit is given in Eq. (A1) in Appendix A.

For a comparison, in the case of a three-dimensional spherical Fermi surface the well known expression¹⁰ for polarization loop $\pi_{3D}(Q)$ results in a prediction for ν_{3D} following from Eq. (19):

$$\nu_{3D}(Q, \omega) \propto \left\{ 1 + \frac{1 - z^2}{2z} \ln \left| \frac{1 + z}{1 - z} \right| \right\}; \text{ where: } z \equiv Q/2p_F. \quad (24)$$

Substituting expressions for ν from eqs. (22) and (24) into modes softening expression Eq. (20) one obtains the dash-dotted and dotted curves in Fig. B for the 1D and 3D holes respectively. The filled circles in Fig. B are obtained from the experimental data² measured in $\text{La}_{1.85}\text{Sr}_{0.15}\text{CuO}_4$ high- T_c cuprate sample ($T_c = 38\text{K}$) by subtracting values of $\omega_{LO}(Q)$ at zero doping from those measured at finite concentration of doped holes. All the curves and data points in Fig. B are normalized by their respective minimal values for each individual set. It is obvious from Fig. B that none of the so far mentioned theoretical curves fits reasonably well the experimental data. The 3D holes produce softening effect that depends on wave-vector Q the way just opposite to the one exhibited by the experimental curve. Simultaneously, phonon coupling to 1D holes on the static stripes, resulting in the self-energy (21), cannot reproduce the measured^{1,2} shallow Q -dependence of the phonon modes softening, that takes place within a sizable interval of momenta comparable with p_F itself.

V. PHONON SELF-ENERGY: 1D HOLES INSIDE DYNAMIC STRIPES

Now we demonstrate that good correspondence with experiment in underdoped cuprates can be achieved by inclusion of an extra massless bosonic propagator with small momentum transfer ($q \ll p_F$) accompanying on-stripe hole-phonon scattering event, as it is indicated by the wavy line in Fig. B. This extra scattering can be ascribed to transversal stripe meandering in the $\{x, y\}$ -plane. Expression for polarization loop $\Pi(Q, i\omega)$, with wavy-line included in accord with Fig. B, looks as follows :

$$\begin{aligned} \text{Re}\Pi(Q, i\omega) = & -\frac{\tilde{g}^2}{\pi} \int_{-\infty}^{\infty} d\epsilon \int dq \{ \text{Img}^R(q, \epsilon) \text{Re}\pi^R(Q - q, \omega - \epsilon) + \\ & \text{Im}\pi^R(Q - q, \epsilon) \text{Reg}^R(q, \epsilon + \omega) \} \coth\left(\frac{\epsilon}{2T}\right); \omega = 2\pi nT, n = 0, \pm 1, \dots, \end{aligned} \quad (25)$$

where momentum q is expressed in the reciprocal lattice units, all energies are expressed in units of ϵ_F , and dimensionless \tilde{g} redefines the coupling constant g , that was introduced in Eqs. (21) and (23) for the case of static stripes. An explicit expression for \tilde{g}^2 is derived below.

Now, the choice of the “meandering propagator” $g^R(k, \omega)$ should be made. A phonon-like propagator has the form:

$$g^R(k, \omega) = \frac{1}{2\omega_k} \left(\frac{1}{\omega - \omega_k + i\Delta} - \frac{1}{\omega + \omega_k + i\Delta} \right), \quad (26)$$

where Δ signifies inverse lifetime of the excitation. Below two cases are considered: underdamped $\omega_k \propto c_\alpha k \gg \Delta$, and overdamped $\omega_k \ll \Delta$, stripe meandering excitations. Before detailing the results, a heuristic derivation of a dimensionless \tilde{g} for the four-leg vertex in Fig. B is in order. This is most easily done using Eq. (B4). The latter equation infers for the case of a small stripe meandering F_q with wave vector q (along the stripe) a dimensionless hole-stripe coupling amplitude $\sim pF_q$, where $F_q \sim \sqrt{\hbar/M\omega_q}$ and $p \sim p_F/\hbar$. Here the property of the Bessel function: $J_1(x \rightarrow 0) \propto x$ at small arguments is used. The dispersion function ω_q enters meandering propagator $g(q, \omega)$ in Eq. (26) and M is “mass” associated with the stripe meandering. Hence, the dimensionless coupling constant \tilde{g} introduced in Eq. (25) equals :

$$\tilde{g}^2 = p_F^2 / (M\epsilon_F) \sim m/M. \quad (27)$$

where m is hole (electron) mass.

A. Underdamped stripe meandering case

First, substitute phonon-like propagator (26) into (25), and use results (A1) and (A2) for the 1D polarization loop $\pi(Q, \omega)$. The real part $\text{Re}\Pi(Q, \omega)$ as function of momentum Q at fixed ω (corresponding to the value ω_{LO} of the softened LO mode in cuprates) proves to be negative (see dashed line in Fig. B), and therefore, softening of the bare phonon band occurs according to explained in detail in the text after Eq. (17). Substitution of the calculated $\text{Re}\Pi(Q, \omega)$ into Eq. (20) gives Q -dependence of the mode softening. The softening value, $\Delta\omega(Q)$, normalized by its maximal (absolute) amount along the calculated curve, $\Delta\omega_0$, is plotted with dashed line in Fig. B. The best fit is shown, that implies $\tau_p^{-1}/\epsilon_F = 1.0$, $c_\alpha = 0.1v_F$ (v_F is the Fermi velocity), $\Delta/\epsilon_F = 0.05$, and meandering wave vector carried by the wavy line in Fig. B obeys : $|k| \leq 0.7p_F$. The discrepancy in the slope of the mode softening as function of Q with the normalized experimental data² (filled circles) for the LO-mode softening in $\text{La}_{1.85}\text{Sr}_{0.15}\text{CuO}_4$ high- T_c cuprate is rather apparent. Since, according to Eq. (27) : $\tilde{g}^2 \sim m/M \sim c_\alpha^2/v_F^2 = 0.01$ for this fit, the more drastic discrepancy with experiment lies in the relative mode softening value. It follows from relation (20) and above estimate of \tilde{g}^2 that :

$$\Delta\omega_{t,L}/\omega_{t,L}^0 \sim (\nu/Q)^2 \approx 0.01, \quad (28)$$

assuming $x_h = 0.15$. This is order of magnitude below the experimental mode softening amount $\sim 0.15^{1,2}$.

B. Overdamped stripe meandering case

In this case, substitution of the calculated $Re\Pi(Q, \omega)$ into Eq. (20) gives Q -dependence that is plotted with solid line in Fig. B. One sees impressive correspondence with experimental data. Again, the best fit is shown, that now implies $\tau_p^{-1}/\epsilon_F = 1.0$, $\Delta/\epsilon_F = 2.0$, and $|k| \leq 0.1p_F$, i.e. describing long-wavelength meandering. Because of the latter choice, the value of “velocity” c_α becomes immaterial, provided it obeys: $c_\alpha \lesssim 10v_F$. Here the relative mode softening value reaches $\Delta\omega_{t,L}/\omega_{t,L}^0 \sim (\nu/Q)^2 \sim 0.1$, that is comparable with experimental softening amount $\sim 0.15^{1,2}$ under condition derived using Eq. (27) :

$$m/M \sim 10. \quad (29)$$

VI. THEORY VS EXPERIMENT: CONSEQUENCES OF THE CORRESPONDENCE

The following picture emerges through the “keyhole” results described above. The “light mass” M in Eq. (29), infiltrated in relation with long-wavelength stripe meandering, could be in principle understood provided the following conditions are fulfilled: i) the stripe meandering is very weakly coupled to the crystal lattice; ii) “light mass” M has electronic origin and is an effective mass/per period (along stripe) of the solitonic domain wall separating neighboring antiphase antiferromagnetic domains of the stripe phase pattern⁹. Next to mention here, is severe suppression of the on-stripe hole quasi-particle strength, since the best fit of the experimental data implies inverse lifetime of the order of the bare Fermi-energy $\tau^{-1} = \epsilon_F$. The transverse meandering vibrations are also strongly damped, as the same fit demands that their inverse lifetime $\Delta = 2\epsilon_F$.

Another important consequence of the results plotted in Fig. B is the implicit value of the Fermi-momentum of the on-stripe holes: $p_F = \pi/2a$, where a is the unit cell spacing along the stripe. Only with this choice the theoretical curve could be successfully superposed on the experimental data^{1,2}. The reason is that $Q = 2p_F$ defines position of zero for the theoretical curves along Q -axis in Fig.B. On the other hand, a weak-coupling consideration using spinful fermionic holes that fill half of the on-stripe sites, leads to the estimate : $p_F = \pi/4a^6$. The discrepancy could be tolerated if one assumes that on-stripe particles interacting with LO phonons are spinless fermions, since in this case their Fermi-momentum p_F^s is twice the spinful one: $p_F^s = 2p_F$. Then, one has to assume that the ARPES experiments in Nd-doped $La_{1.28}Nd_{0.6}Sr_{0.12}CuO_4$ ⁶, probably, register already “spin-dressed” (spinful) fermions, since the “holly cross” pattern of the occupied 1D electron states gives $2p_F = \pi/2a$ for the distance between parallel pieces of the quasi 1D “Fermi surface”. The latter is ascribed to 1D motion of holes along array of the parallel stripes.

ACKNOWLEDGEMENTS

The author acknowledges important communications with Alan Bishop and Jan Zaanen concerning facts related with phonon softening and concepts of dynamic stripe-phase in high- T_c cuprates.

APPENDIX A: PHONON SELF-ENERGY CALCULATIONS

After the substitution $\tanh(\epsilon/2T) \rightarrow \text{sign}\epsilon$, a direct integration over variable ϵ in the expression (22) leads to the following answer:

$$\nu(Q, \omega) = \gamma \frac{1}{2\pi} \int dp \left\{ \frac{1}{\tilde{\epsilon}_1 - \tilde{\epsilon}_2 - \omega} \left[\arctan \left(\frac{\tau^{-1}}{\tilde{\epsilon}_2 + \omega} \right) - \arctan \left(\frac{\tau^{-1}}{\tilde{\epsilon}_1} \right) - \arctan \left(\frac{\tau^{-1}}{\tilde{\epsilon}_1 - \omega} \right) + \arctan \left(\frac{\tau^{-1}}{\tilde{\epsilon}_2} \right) \right] - \frac{1}{(\tilde{\epsilon}_1 - \tilde{\epsilon}_2 - \omega)^2 + 4\tau^{-2}} [(\tilde{\epsilon}_1 - \tilde{\epsilon}_2 - \omega) \times \right.$$

$$\left[\arctan\left(\frac{\tau^{-1}}{\tilde{\epsilon}_2 + \omega}\right) + \arctan\left(\frac{\tau^{-1}}{\tilde{\epsilon}_1}\right) - \arctan\left(\frac{\tau^{-1}}{\tilde{\epsilon}_1 - \omega}\right) - \arctan\left(\frac{\tau^{-1}}{\tilde{\epsilon}_2}\right) \right] + \tau^{-1} \ln\left(\frac{(\tilde{\epsilon}_2 + \omega)^2 + \tau^{-2}}{\tilde{\epsilon}_1^2 + \tau^{-2}} \frac{(\tilde{\epsilon}_1 - \omega)^2 + \tau^{-2}}{\tilde{\epsilon}_2^2 + \tau^{-2}}\right) \Big\} \}. \quad (A1)$$

In accord with the formula (19) for the wave vector ν expression (A1) gives (modulo constant prefactor) the real part of the polarization loop, $Re\pi^R(Q, \omega)$. Simultaneously, the imaginary part $Im\pi^R(Q, \omega)$, derived from Eq. (21), equals:

$$Im\pi^R(Q, \omega) = \frac{g^2}{\varepsilon_F V_0} \frac{1}{2\pi} \int dp \left\{ \frac{\tau^{-1}}{(\tilde{\epsilon}_1 - \tilde{\epsilon}_2 - \omega)^2 + 4\tau^{-2}} \left[\arctan\left(\frac{\tau^{-1}}{\tilde{\epsilon}_2 + \omega}\right) + \arctan\left(\frac{\tau^{-1}}{\tilde{\epsilon}_1}\right) - \arctan\left(\frac{\tau^{-1}}{\tilde{\epsilon}_1 - \omega}\right) - \arctan\left(\frac{\tau^{-1}}{\tilde{\epsilon}_2}\right) \right] + \frac{\tau^{-2}}{(\tilde{\epsilon}_1 - \tilde{\epsilon}_2 - \omega)[(\tilde{\epsilon}_1 - \tilde{\epsilon}_2 - \omega)^2 + 4\tau^{-2}]} \left[\ln\left(\frac{(\tilde{\epsilon}_2 + \omega)^2 + \tau^{-2}}{\tilde{\epsilon}_1^2 + \tau^{-2}}\right) + \ln\left(\frac{(\tilde{\epsilon}_1 - \omega)^2 + \tau^{-2}}{\tilde{\epsilon}_2^2 + \tau^{-2}}\right) \right] \right\}, \quad (A2)$$

The following choice of $\arctan(x)$ branches is adopted:

$$\arctan(x \rightarrow \pm\infty) = \frac{\pi}{2}; \quad \arctan(x \rightarrow 0^-) = \pi; \quad \arctan(x \rightarrow 0^+) = 0. \quad (A3)$$

Here: $\tilde{\epsilon}_1 \equiv \tilde{\epsilon}(p)$ and $\tilde{\epsilon}_2 \equiv \tilde{\epsilon}(p + Q)$, and all energies and inverse life-times are expressed in units of the bare Fermi-energy ε_F of the on-stripe holes. The difference between τ_p and τ_{p+Q} is neglected.

APPENDIX B: STRIPE MEANDERING EFFECT ON 1D HOLE MOTION

Consider a simple on-stripe “plane wave” function $\Psi_p(x)$ of electron (hole) moving along a stripe (i.e. dynamically curved 1D space), that is preferentially oriented parallel to the x -axis. The actual length $L(x, t)$ of the dynamically curved stripe equals (see e.g.⁴):

$$L(x, t) = \int_0^x dx' \sqrt{1 + (\partial_{x'} Y(x', t))^2} + L(0), \quad (B1)$$

where $Y(x, t)$ describes space(x) and time(t)-dependent deviation of the stripe from the straight line. Assuming for simplicity that $(\partial_{x'} Y(x', t))^2 \ll 1$ and making expansion of the square root one finds:

$$\Psi_p(x) = \exp(ipL(x, t)) \approx \exp\{ip(L(0) + x) + ipF(x, t)\}; \quad (B2)$$

$$F(x, t) = \frac{1}{2} \int_0^x dx' (\partial_{x'} Y(x', t))^2 = F_0(t)x + \sum_q F_q \sin(qx - \omega_q t + \theta_q) \quad (B3)$$

In (B3) the stripe-line length is expanded over a harmonics, each one being characterized with wave vector q , frequency ω_q , and phase θ_q of the corresponding transverse vibration mode of the stripe. Considering separately effect on the wave-function (B2) of each particular q -term from the sum in (B3), it is convenient to use representation of $\exp\{ipF \sin(x)\}$ via Bessel functions J_n of integer order n :

$$\Psi_p(x) \approx \exp\{ip[L(0) + x(1 + F_0(t))]\} \prod_q \sum_n J_n(pF_q) \exp\{in(qx - \omega_q t + \theta_q)\} \quad (B4)$$

Hence, according to Eq.(B4) a long-wavelength vibration of the stripe causes (forward) scattering $p \rightarrow p + nq$ of the on-stripe holes and $J_n(pF_q)$ gives its amplitude (scattering matrix element).

- ¹ R.J. McQueeney et al., Phys. Rev. Lett. vol.82,628 (1999).
- ² L. Pintschovius and M. Braden, Phys. Rev. B 60,R15039 (1999).
- ³ I. Martin et al., Phys. Rev. B 70, 224512 (2004).
- ⁴ S.A. Kivelson, E. Fradkin, V.J. Emery, Nature vol. 393, 550 (1998).
- ⁵ S.I. Mukhin, Dynamic stripe-phase and quasi one-dimensionality of electron-phonon coupling in high-T_c cuprates, Proc. Int. Conf. "From Solid State to Biophysics II: Role of Inhomogeneities in Solid, Soft and Bio-Matter, Dubrovnik, Croatia, 26th June-2nd July, 2004.
- ⁶ X.J. Zhou et al., Science vol. 286, 268 (1999).
- ⁷ H. Kleinert, Gauge Fields in Condensed Matter, vol.II: Stresses and Defects, Differential Geometry, Crystal Defects, World Scientific, Singapore, 1989.
- ⁸ J.M. Tranquada et al., Nature vol. 375, 561 (1995).
- ⁹ J. Zaanen and O. Gunnarson, Phys. Rev B 40, 7391 (1989).
- ¹⁰ A.A. Abrikosov, L.P. Gor'kov, I.E. Dzyaloshinski, Methods of Quantum Field Theory in Statistical Physics, Dover Publications, New York, 1963.

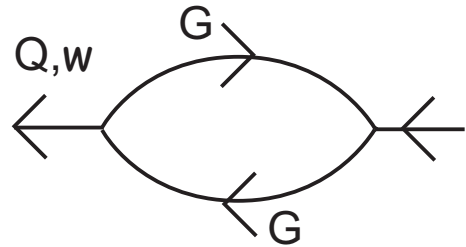


FIG. 1. Phonon self-energy $\pi(Q, \omega)$: single-loop diagram for 1D on-stripe holes. Dot is electron(hole)-lattice coupling vertex, the thin lines are Green's functions $G(p, \epsilon)$ of the 1D hole possesing momentum p along the stripe direction.

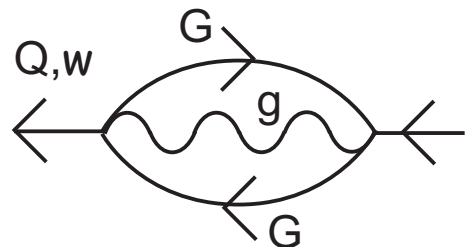


FIG. 2. Same as Fig. B, but with wavy line for stripe meandering propagator $g(q, \omega)$.

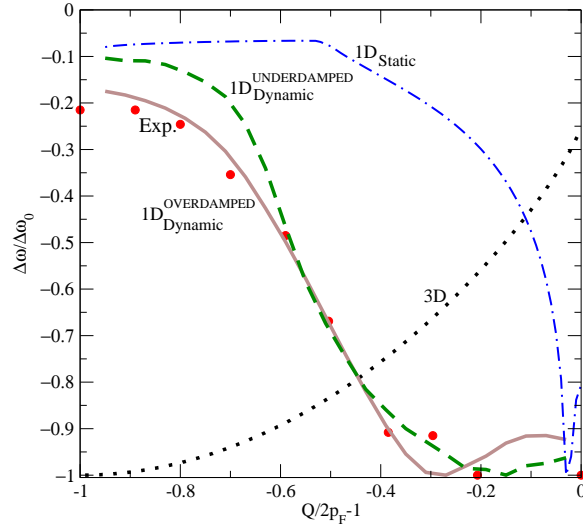


FIG. 3. Softening of the phonon band. Filled circles: experimental data by [2] for $\text{La}_{1.85}\text{Sr}_{0.15}\text{CuO}_4$, $T_c = 38K$; solid line: 1D holes on meandering stripe, using Fig. B with wavy line (26) in the overdamped case; dashed line: the same as solid line, but with (26) in underdamped case; dash-dotted line: 1D holes on static stripe, Fig. B; dotted line: 3D holes, using Fig. B with 3D fermionic propagators G . $\Delta\omega_0$ normalizes all curves at their minima to -1 .

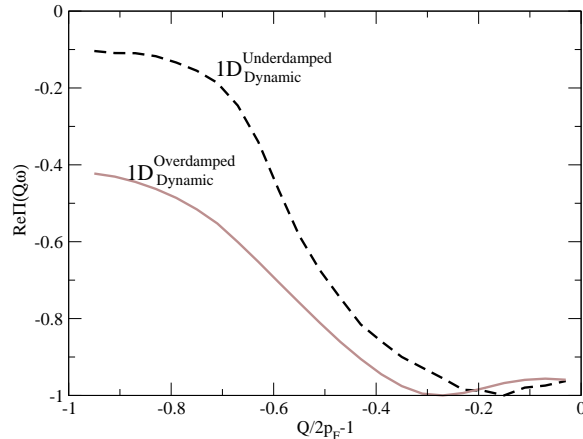


FIG. 4. Polarization $Re\Pi(Q, \omega)$ as function of momentum Q at fixed $\omega = 0.1\varepsilon_F$. Solid line is calculated with overdamped phonon-like propagator Eq. (26). Dashed line is for underdamped case. All curves are normalized to -1 at their minima.